

## Fabrication of multiphasic and regio-specifically functionalized PRINT<sup>®</sup> particles of controlled size and shape

H Zhang<sup>1</sup>, J K Nunes<sup>1</sup>, S E A Gratton<sup>1</sup>, K P Herlihy<sup>1</sup>,  
P D Pohlhaus<sup>2</sup> and J M DeSimone<sup>1,3,4</sup>

<sup>1</sup> Department of Chemistry, University of North Carolina at Chapel Hill,  
Chapel Hill, NC 27599, USA

<sup>2</sup> Liquidia Technologies, PO Box 110085, Research Triangle Park,  
NC 27709, USA

<sup>3</sup> Department of Chemical and Biomolecular Engineering,  
North Carolina State University, Raleigh, NC 27695, USA

E-mail: [desimone@unc.edu](mailto:desimone@unc.edu)

*New Journal of Physics* **11** (2009) 075018 (16pp)

Received 4 February 2009

Published 31 July 2009

Online at <http://www.njp.org/>

doi:10.1088/1367-2630/11/7/075018

**Abstract.** Using Particle Replication In Nonwetting Templates (PRINT<sup>®</sup>) technology, multiphasic and regio-specifically functionalized shape-controlled particles have been fabricated that include end-labeled particles via post-functionalization; biphasic Janus particles that integrate two compositionally different chemistries into a single particle; and more complex multiphasic shape-specific particles. Controlling the anisotropic distribution of matter within a particle creates an extra parameter in the colloidal particle design, providing opportunities to generate advanced particles with versatile and tunable compositions, properties, and thus functionalities. Owing to their robust characteristics, these multiphasic and regio-specifically functionalized PRINT particles should be promising platforms for applications in life science and materials science.

<sup>4</sup> Author to whom any correspondence should be addressed.

**Contents**

<b>1. Introduction</b>	<b>2</b>
<b>2. Experimental</b>	<b>3</b>
2.1. Materials . . . . .	3
2.2. The PRINT process . . . . .	3
<b>3. Regio-specifically functionalized PRINT particles</b>	<b>4</b>
3.1. Chemical grafting . . . . .	5
3.2. Metal deposition . . . . .	7
<b>4. Janus particles</b>	<b>8</b>
<b>5. Multiphasic and regio-specifically functionalized particles</b>	<b>12</b>
<b>6. Conclusions</b>	<b>13</b>
<b>Acknowledgments</b>	<b>14</b>
<b>References</b>	<b>15</b>

**1. Introduction**

Advances in the field of nanotechnology, especially as it pertains to the design of nanometer- and micron-sized particles, have allowed for the fabrication of particles with sophisticated moieties, such as delicate cargo and surface-bound targeting ligands [1, 2]. However, in general, the distinct chemical species that compose a particle isotropically distribute in the particle to form either chemically disordered alloys or core-shell layered structures [3]. Controlling the distribution of matter in the particles allows for an extra parameter in the design process beyond the fundamental size and shape considerations, especially when the overall size and shape of the particle is controlled. It is advantageous to fabricate anisotropically phase-separated multiphasic particles owing to the resulting unique attributes not possible in single component or isotropically distributed multicomponent particles. These attributes include the ability to simultaneously utilize the different functions incorporated into the particle such as mechanical, chemical, optical, biological, electrical and magnetic properties as well as the ability to function as multiple component carriers for drug delivery. Also, distinct functional ligands can be anisotropically arranged on the surface of particles, thus leading to unique properties tailored for various material and life science applications. Such behavior affords opportunities to create revolutionary new materials through combinations of different functionalities [4].

Using Particle Replication In Nonwetting Templates (PRINT) technology, it has been demonstrated that monodisperse, shape-specific particles can be readily fabricated with controlled size, shape, matrix composition, cargo and surface chemistry [2], [5]–[13]. The fundamental distinction between PRINT and other imprint lithography techniques [14]–[16] lies in the use of a highly fluorinated elastomer as the molding material in place of silicones, the dominant material in this field. As perfluoropolyether (PFPE) elastomers have very low surface energies, the mold cavities can be selectively filled without wetting the land area between cavities, thus fabricating discrete particles without an interconnecting ‘flash’ or ‘scum’ layer. The low surface energy also facilitates easy removal or harvesting of particles from the mold. Furthermore, organic liquids do not swell PFPE elastomers as they do silicones, so a wide range of particle compositions can be explored. PRINT allows the fabrication of precisely

defined micro- and nano-particles with control over particle size (20 nm to >20 microns), shape (spheres, cylinders, discs, toroids, etc), chemical composition (organic/inorganic and solid/porous), cargo (magnetite, biosensors, therapeutics, proteins, oligonucleotides, siRNA and imaging agents), modulus (stiff/deformable), and surface chemistries (antibodies, poly(ethylene glycol) chains and metal chelators), including the spatial distribution of ligands on the particle. Our previous studies have shown the ability to make precisely defined PRINT particles from a wide range of chemistries including different hydrogel materials, biodegradable polylactides, titania, barium titanate, tin oxide, etc [2], [5]–[13]. PRINT is the only particle technology that can create truly engineered particles from such a diverse range of chemistries in form factors that include free-flowing powders, isotropic and external field (electric and magnetic) aligned colloidal dispersions, and two- and three-dimensional arrays of nanoparticles. In this work, we introduce novel methods to fabricate complex PRINT particles that contain anisotropic chemistries, and thus greatly broaden the versatility of PRINT technology as a platform for materials and life sciences.

## 2. Experimental

### 2.1. Materials

The following reagents were used as received: 2,2-diethoxyacetophenone (DEAP, Aldrich), 2-aminoethyl methacrylate hydrochloride (AEM, Aldrich), fluorescein *o*-acrylate (Aldrich), dimethyl sulfoxide (DMSO, Aldrich), 1-hydroxycyclohexyl phenyl ketone (HCPK, Aldrich), poly(ethylene glycol) monomethyl ether monomethacrylate ( $M_n$  1000 g mol<sup>-1</sup>, PEG<sub>1000</sub>, Polysciences), pH 8.60 borax buffer (Ricca Chemical), polystyrene ( $M_n$  10 500 g mol<sup>-1</sup>, Polymer Standards Service), chlorobenzene (Aldrich) and N-hydroxysuccinimide (NHS)-rhodamine (Pierce). Trimethylolpropane triacrylate (Aldrich), trimethylolpropane ethoxylate triacrylate ( $M_n$  428 g mol<sup>-1</sup> and 912 g mol<sup>-1</sup>, PEG<sub>428</sub> triacrylate and PEG<sub>912</sub> triacrylate, respectively, Aldrich), lauryl acrylate (Aldrich) and acrylic acid (Aldrich) were de-inhibited by passing through a column of alumina. Cyanoacrylate adhesive (Zap CA PT-08, Pacer Technologies) was used as received. The PFPE prepolymer resin (Fluorocur<sup>TM</sup>, Liquidia Technologies, Inc.) was mixed with 0.1wt% DEAP photoinitiator before use. The untreated side of poly(ethylene terephthalate) (PET) sheets (Melinex 453, Tekra) was used for monomer distribution and removal. Liquidia Technologies Inc. provided a 200 mm polymer replica master with hexagonal close-packed hexnut features (2.5  $\mu$ m flat-to-flat, 1  $\mu$ m height) spaced by 1.5  $\mu$ m.

Scanning electron microscopy (SEM) imaging was accomplished on a Hitachi model S-4700. Zeta potential was measured using a ZetaPlus Zeta Potential Analyzer (Brookhaven Instruments Corporation). Confocal micrographs were captured on an Olympus FV500 confocal laser scanning microscope (Olympus Co Ltd). Palladium/gold (Pd/Au) alloy was deposited using a sputter coater (Model 108 Auto Sputter Coater, Cressington Scientific Instruments). Fluorescence and optical images were obtained using a Zeiss Axioskop 2 MAT incident light microscope fitted with an AxioCam MR digital camera.

### 2.2. The PRINT process

The PRINT process has been described extensively elsewhere [6, 8, 9, 13]. Briefly, 5–10 ml Fluorocur<sup>TM</sup> resin was poured onto a patterned silicon wafer or patterned polymer

replica, purged with nitrogen ( $N_2$ ) and cured via UV irradiation for 3 min ( $\lambda_{\max} = 365$  nm,  $P \geq 20$  mW cm $^{-2}$ ). After curing, the PFPE mold was removed from the template. A small aliquot of a monomer solution was then deposited on the surface of the mold and spread uniformly by laminating onto a PET sheet. The PET sheet was then peeled back effectively removing the excess monomer from the land areas and leaving the mold cavities filled with monomer solution. The filled mold was then purged with dry  $N_2$  and subsequently exposed to UV-light for 3 min under continued purge. At this step, the exposed particle surfaces were subjected to the post-functionalization processes described in detail in the following sections. To harvest the particles, the filled mold was hand-laminated over a small aliquot (100  $\mu$ l) of cyanoacrylate on a glass slide and the cyanoacrylate was allowed to moisture cure. The mold was then peeled back from the glass slide leaving an array of particles firmly bound to the slide by the polycyanoacrylate. The particles were then rinsed with filtered acetone to remove them from the glass slides and collected in 50 ml falcon tubes. To purify the particles, the suspension was centrifuged, the supernatant removed, and then the particle pellet was redispersed in fresh acetone by vortexing. This was repeated at least 10 times to remove the dissolved adhesive.

### 3. Regio-specifically functionalized PRINT particles

It is highly advantageous to the field of colloidal science to develop synthetic methods for creating particles where each particle possesses multiple, spatially defined surface chemistries. In fact, there has been such great interest in nanoparticles with anisotropic shapes and chemistries that efforts have been made toward the development of a unifying conceptual framework to define the myriad of potential particle classes. Glotzer and Solomon outlined the following key anisotropy ‘dimensions’ to describe the particles’ attributes: surface coverage (patchiness), aspect ratio, faceting, pattern quantization, branching, chemical ordering, shape gradient and roughness [17]. The potential applications of such anisotropic particles are far-reaching. In particular for colloidal self-assembly, it is a powerful tool to be able to decorate the surface of particles with predetermined ‘instructions’ for self-assembly [18]. Another arena in which particles with anisotropic chemistries can potentially play a critical role is in medical discovery, screening and diagnostics [19, 20]. These particles can be synthesized with encoded information on their surfaces to address multiplexing needs.

Over the years, this emerging field of ‘patchy’ particles, where the patches are attractive interaction sites [21], has benefited from the numerous advances in the synthesis of particles with anisotropic surface chemistries [22]–[28]. Solution-based batch processes have been developed that allow for the fabrication of dipolar and amphiphilic spherical silica particles by trapping the particles at the interface of an oil–water emulsion, solidifying the oil, then chemically modifying the exposed particle surface [24]. Two-dimensional synthetic methods have also been developed where a layer of the particles is prepared on a substrate and a partial protective layer is applied, so that only the unprotected surfaces were chemically and/or physically modified [22, 23, 25, 27]. Among all the novel strategies developed, the experimental challenge has been, and continues to be, accomplishing the particle synthesis in a uniform, reproducible, and scaleable fashion, while maintaining complete control over the particle properties.

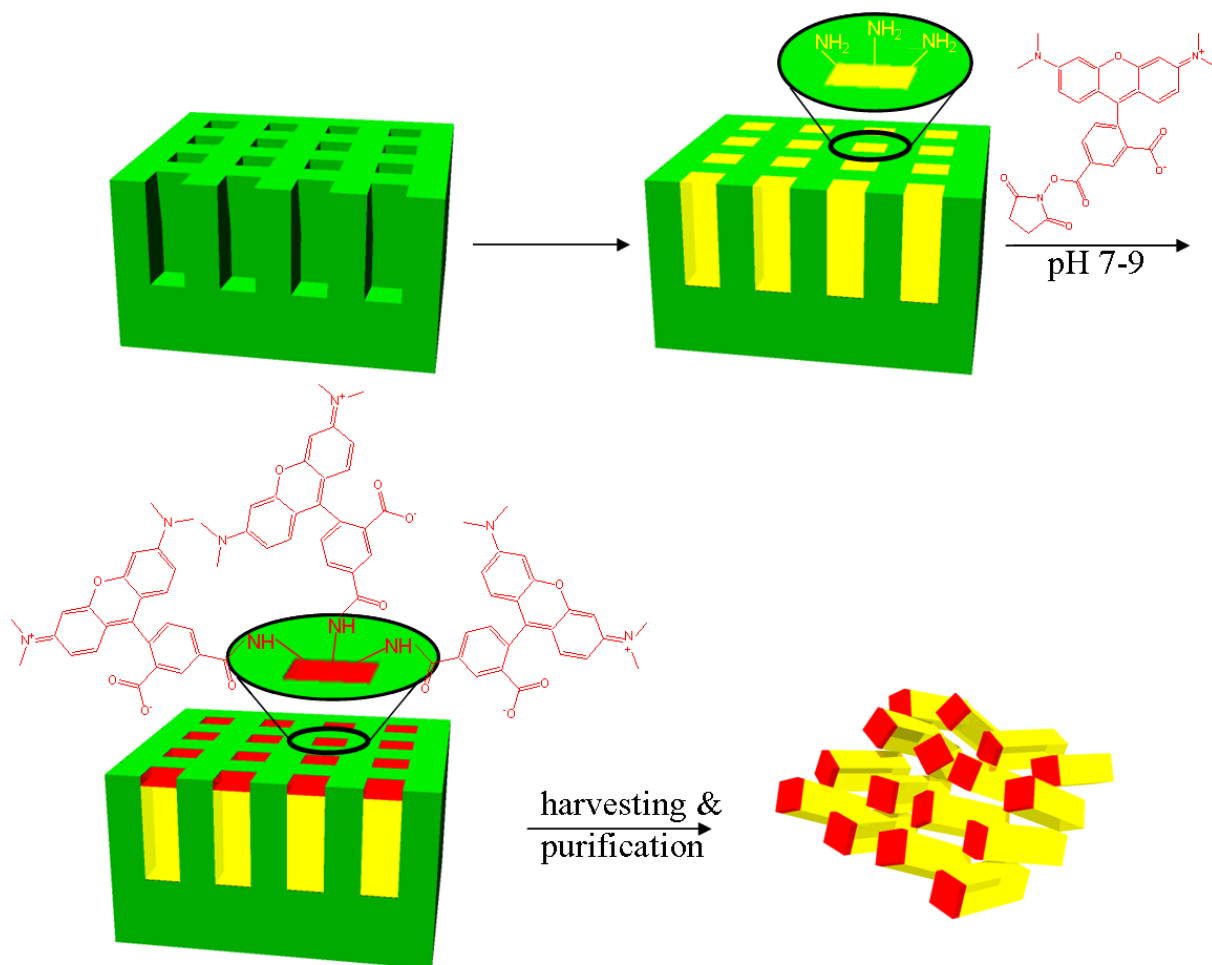
We have previously demonstrated the ability to uniformly functionalize the surface of PRINT particles by incorporating into the bulk of the particle reactive handles that are available on the particle surface after fabrication. For example, primary amine functional monomers have

been incorporated into the bulk of the particles. These primary amine handles present in the particle then allow the particles to be efficiently functionalized with NHS-ester reagents to graft moieties such as biotin which can then subsequently be used to bind the protein avidin to the particle surface through the formation of stable amide bonds. This fabrication process results in the isotropic functionalization of the entire particle surface [12]. Here we discuss the anisotropic chemical functionalization of anisotropically shaped PRINT particles. One advantage of the PRINT process is that after the particles are fabricated, while the particles are still in the mold, one face of the particle is left exposed. Thus, that surface can be chemically modified exclusive of the other particle faces that are masked by the mold resulting in a regio-specifically functionalized particle where two surface chemistries are spatially isolated on the particle.

### 3.1. Chemical grafting

One example of chemical anisotropy was achieved by chemically grafting to one face of the particles. Two particle shapes were studied:  $2 \times 2 \times 6 \mu\text{m}$  rectangular prisms and  $3 \mu\text{m}$  hexnut particles (vertex to vertex distance =  $3 \mu\text{m}$ , height =  $1 \mu\text{m}$ , fenestration diameter =  $1 \mu\text{m}$ ). The PRINT particles were composed of 67 wt% of the crosslinker PEG<sub>428</sub> triacrylate, 20 wt% PEG<sub>1000</sub> monomethyl ether monomethacrylate, 10 wt% of the primary amine monomer AEM, 2 wt% of the fluorescence monomer fluorescein *o*-acrylate used for imaging, and 1 wt% of the photoinitiator DEAP. The AEM functioned as the chemical handle in this composition. After UV curing, the full mold of particles was inverted into a solution of buffered NHS-rhodamine and allowed to react for 90 s. Scheme 1 illustrates this process. The molds were then thoroughly rinsed with water, dried, and harvested using polycyanoacrylate as a sacrificial adhesive. The adhesive was then dissolved in acetone and the particles were collected and purified with repeated washes in acetone. In figure 1(a), the regio-specifically functionalized  $2 \times 2 \times 6 \mu\text{m}$  particles are shown on polycyanoacrylate where a small drop of acetone was applied to collapse the particle array; the purified particles are shown in figure 1(b). In figure 1(c) harvested regio-specifically functionalized hexnut particles on polycyanoacrylate are displayed where a drop of acetone has been used to disperse the particles; the purified hexnuts are shown dispersed in water in figure 1(d). When imaged with fluorescence microscopy the particles appeared green because of the fluorescein *o*-acrylate present in the bulk of the particle and the reacted particle face was clearly identified by the red fluorescence of the surface-bound rhodamine dye.

The surface modification was also evident from zeta potential measurements where the unmodified  $2 \times 2 \times 6 \mu\text{m}$  particles possessed a zeta potential of  $+31 \pm 2 \text{ mV}$  while the surface functionalized particles had a zeta potential of  $-16 \pm 3 \text{ mV}$ . Our previous work has demonstrated that this particle composition generally yields positively charged particles, though once the surface amine groups have reacted with acetic anhydride, the particle charge switches to negative values [6]. Thus, it follows that the regio-specifically functionalized particles should possess a positive surface potential except at the modified surface, which was negative. This was corroborated by *in vitro* screens of the end-functionalized  $2 \times 2 \times 6 \mu\text{m}$  prisms. The particles were observed to associate with the cellular membrane of human cervical carcinoma epithelial (HeLa) cells such that the positively charged surfaces of the particles were membrane-bound while the negatively charged surface was positioned furthest from the cellular membrane (figure 2). Given the negatively charged nature of the cell membrane due to the presence of proteoglycans on the surface, the electrostatic interactions between



**Scheme 1.** Reaction scheme for the anisotropic functionalization of primary amine-containing particles in the mold with NHS-rhodamine.

the positively charged surfaces of the particles and the negatively charged membrane were anticipated.

The ability to anisotropically functionalize particles in a controlled site-specific manner adds a new level of control for the design of effective carriers in nanomedicine for the treatment of disease. Early *in vitro* results suggest an enhanced internalization of rod-like particles over more symmetrical nanoparticles having identical particle matrix compositions and roughly equal particle volumes. Moreover, it was found that PRINT particles use multiple pathways of endocytosis for internalization into a cell and that a significant reduction of particle internalization occurred when the particles had a negative zeta potential versus particles having a positive zeta potential [6]. With this new control over surface chemistry, a new design parameter has unfolded, beyond size and shape, allowing for more in depth studies to be conducted to monitor the effect of directed end-on internalization of anisotropic particles to learn the effects of controlled entry into cells on both targeting efficiencies as well as the modes of endocytosis.



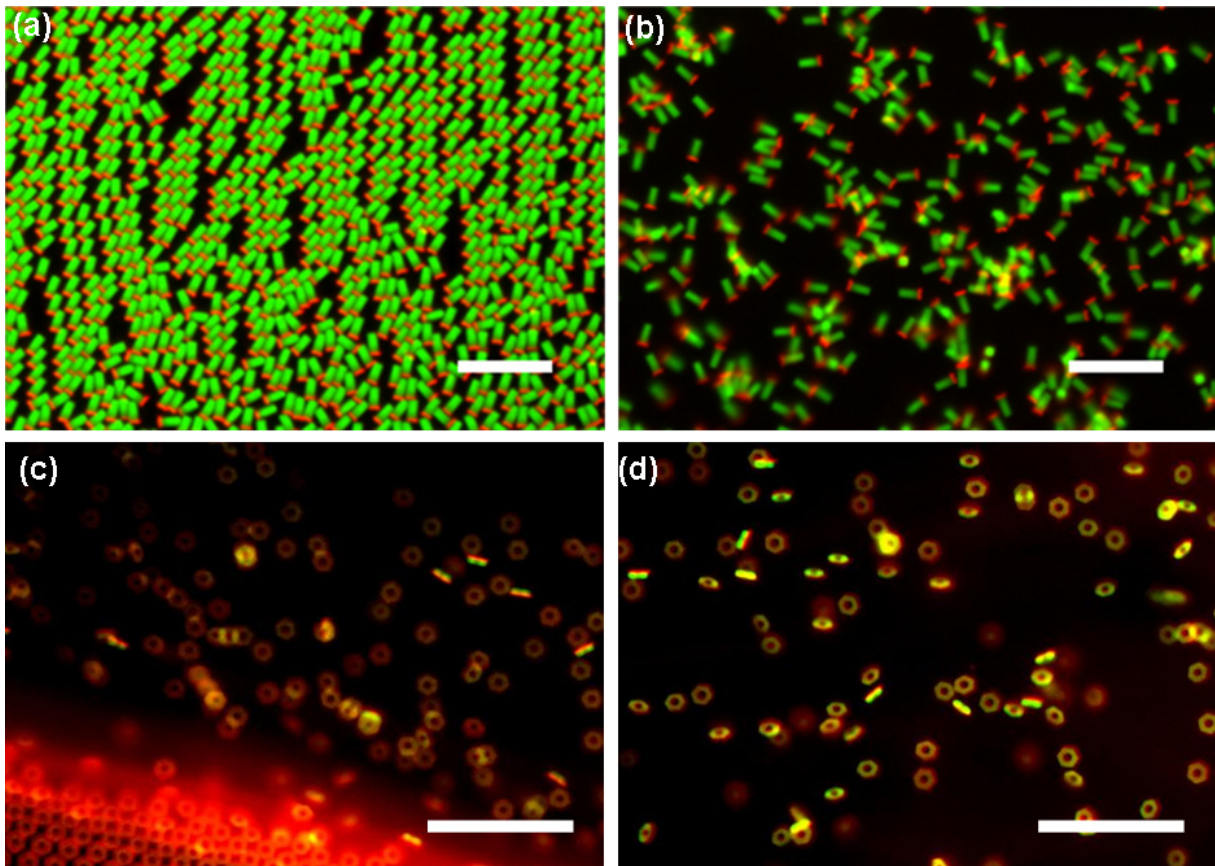


**Figure 1.** Fluorescence images of regio-specifically functionalized PRINT particles where (a) shows  $2 \times 2 \times 6 \mu\text{m}$  regio-specifically functionalized rectangular prisms collapsed on polycyanoacrylate, (b) the purified and dried regio-specifically functionalized prisms, (c) regio-specifically functionalized  $3 \mu\text{m}$  hexnuts on polycyanoacrylate with acetone and (d) the purified regio-specifically functionalized hexnuts. The scale bars represent  $20 \mu\text{m}$ .

### 3.2. Metal deposition

Another simple strategy for achieving chemical anisotropy on a particle surface is through the selective vapor deposition of a metal. In addition to providing a new surface for chemical functionalization [29], the metal surface of the particle can also act as a catalytic site for chemical reactions. For example, Sundararajan *et al* [30] showed that platinum–gold rods can be self-propelled via the catalytic decomposition of hydrogen peroxide and can transport polystyrene microspheres through solution. To prepare metal-capped PRINT particles, 10 nm of a Pd/Au alloy was sputtered onto the surface of a filled rectangular prism mold. After coating, the particles were harvested with polycyanoacrylate and purified. The metallic ends of the particles were visualized using SEM. The metal-coated surfaces appear very bright on the particles (figure 3(a)). Furthermore, energy dispersive x-ray spectroscopy (EDS) analysis confirmed the presence of the metal alloy on the single end. Spot scans along the length of the coated particles indicated the presence of the elements carbon and oxygen along the body of the particles; however, gold and palladium were identified only on the coated ends (figure 3(b)).

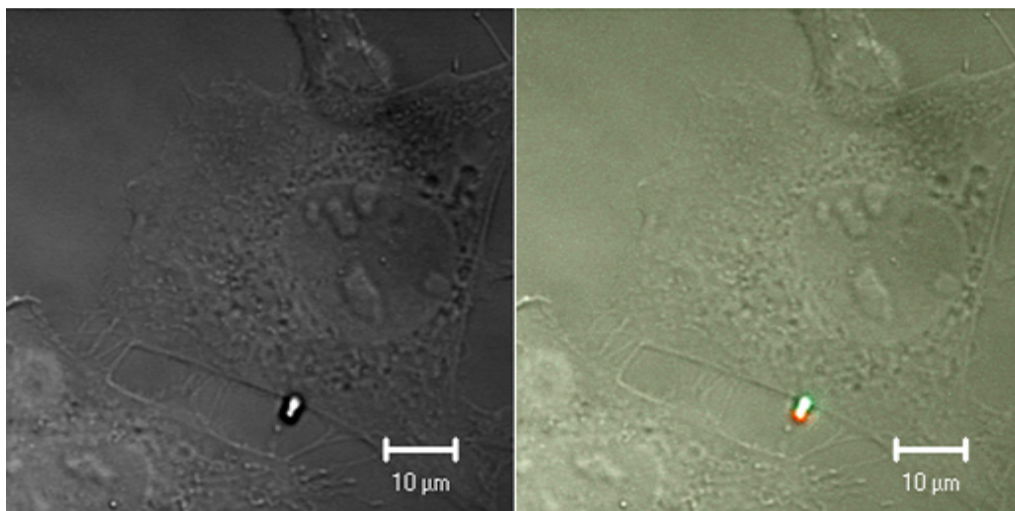


**Figure 2.** Confocal micrographs of  $2 \times 2 \times 6 \mu\text{m}$  regio-specifically functionalized PEG particles interacting with HeLa cells. The positively charged particle surface (green) interacted with the negatively charged membrane of the cells.

#### 4. Janus particles

In Roman mythology, Janus was the god of gates, doors, doorways, beginnings and endings. As he had received from the god Saturn the gift to see both the future and the past, Janus was usually depicted with two faces looking in opposite directions. Janus particles were first reported by Casagrande *et al* [31] in 1989. In their work, glass beads were embedded halfway in a plastic and then silanated on the accessible side. De Gennes was one of the first scientists to use the term Janus. On the occasion of his Nobel lecture in 1991, de Gennes referred to ‘Janus grains’ as those that have two sides: one apolar and the other polar, just like the god Janus had two faces [32].

In recent years, Janus particles have become an emerging new direction of colloidal structures and research interest from various areas ranging from medicine, biochemistry, and physics to colloidal chemistry. Owing to their unique anisotropic characteristics, Janus particles have demonstrated feasibility or are considered very promising candidates with respect to numerous applications: their asymmetric interactions can induce self-assembly [33]; Janus particles with electrical anisotropy can orientate in an electric field and thus switchable devices and electronic displays could be created [34]; by combining a hydrophobic hemisphere with a hydrophilic one, amphiphilic Janus particles can stabilize water–oil emulsions better than homogeneous particles [35]; and biocompatible polymer-based Janus particles can be useful for life science, such as bifunctional carriers for drug delivery and molecular imaging [36]. So far, the top selective surface modification of precursor isotropic particles, spherical ones in the most general case, has been the most intuitive and also the most common approach leading to Janus particles [4, 37]. In this work, we introduce a novel pathway to fabricate size and shape specified non-spherical monodisperse PRINT particles that are composed of different blocks. Our Janus particles are composed of blocks that differ in matrices, in contrast to most other Janus particles that are only functionalized on the surface; therefore these particles can be expected to exhibit improved properties and more robust performance.



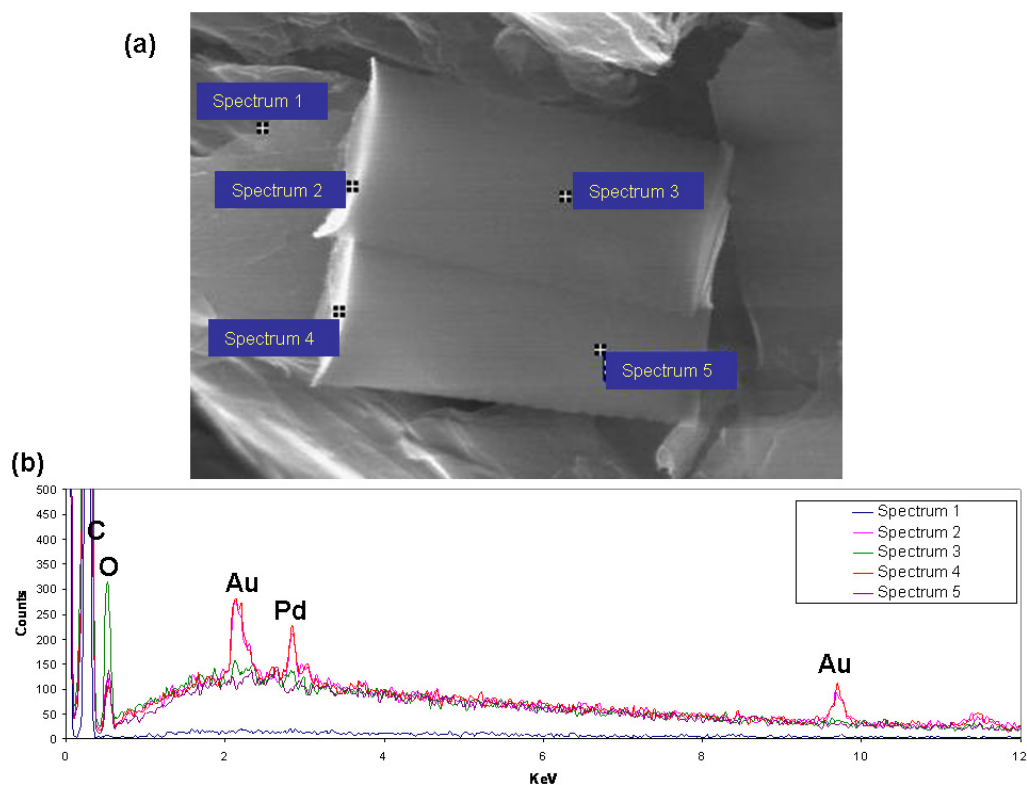
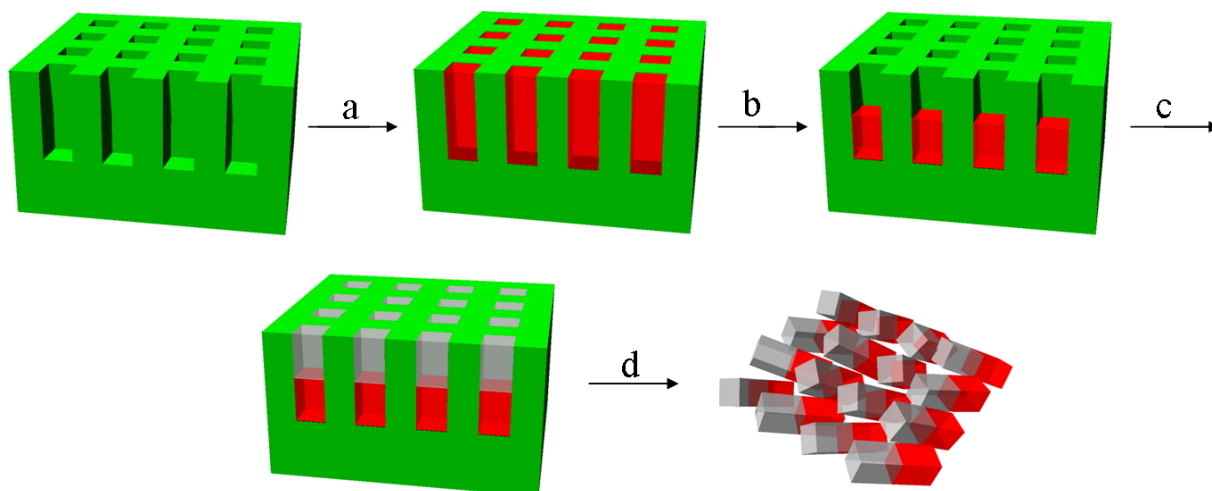


**Figure 3.** (a) SEM image of two  $2 \times 2 \times 6 \mu\text{m}$  metal-capped rectangular prisms on a graphite pin stub, where the indicated regions were scanned with an EDS detector and (b) EDS spectra from different scanned regions. Scan 1 is of the graphite pin background. Scans 2 and 4 are of the particle functionalized end and clearly show the presence of gold and palladium while scans 3 and 4 of the particle body do not show any evidence of metals being present.

PRINT is a ‘top-down’ method for the fabrication of particles; however, to fabricate Janus particles, a ‘bottom-up’ strategy is also employed. As depicted in scheme 2, one photo-curable monomer solution diluted in a volatile solvent is first filled into the mold. Upon evaporation of the volatile solvent the concentrated liquid will shrink to the bottom of the cavity due to the capillary effect. The liquid is then partially photo-cured by exposure to a low density UV source for a short exposure time resulting in a tacky surface. Finally, a second photo-curable monomer solution that is chemically distinct from the first is filled into the mold and completely cured along with the bottom portion, resulting in a particle composed of two chemically distinct blocks. By varying the compositions of the two monomer solutions Janus particles possessing different properties can be fabricated.

To demonstrate this proof of concept, two types of Janus particles were fabricated using PRINT technology: one type was amphiphilic by combining a hydrophobic block with a hydrophilic block, the other was electrostatically anisotropic or dipolar by combining a positively charged block with a negatively charged block. The compositions of the monomer solutions are tabulated in tables 1 and 2. Both types of particles fabricated were  $2 \times 2 \times 6 \mu\text{m}$  rectangular prisms. Isopropanol was used as a volatile solvent to dilute the first monomer



**Scheme 2.** Fabrication of Janus particles using PRINT technology: (a) one monomer solution that has been diluted by a volatile solvent is filled into the mold; (b) after evaporation of the solvent, the remaining liquid is partially photo-cured; (c) the other monomer solution is filled, all liquids are completely cured and (d) Janus particles are obtained after harvesting and purification.

**Table 1.** The compositions of hydrophobic–hydrophilic Janus particles. The cross-linkers in both phases were chosen according to their philicities. DMSO was added to dissolve the initiator and fluorophore.

	Wt%	Function
Bottom hydrophobic block in the mold		
Trimethylolpropane triacrylate	47	Cross-linking agent
Lauryl acrylate	50	Hydrophobe
Fluorescein <i>o</i> -acrylate	2	Fluorophore
HCPK	1	Initiator
DMSO	10 $\mu$ l/100 mg monomer	Solvent
Isopropanol	200 $\mu$ l/100 mg monomer	Volatile solvent
Top hydrophilic block in the mold		
PEG <sub>912</sub> triacrylate	49	Cross-linking agent
PEG <sub>1000</sub>	50	Hydrophile
HCPK	1	Initiator
DMSO	10 $\mu$ l/100 mg monomer	Solvent

solution. After evaporation of the isopropanol, the remaining monomer was partially photo-cured via UV irradiation with an appropriate exposure time depending on the monomer species and the cross-linker content in the composition and the miscibility of the monomer compositions of the two blocks. Under curing the first monomer block prevents permeation between the two blocks but also allows the two blocks to be physically conjoined. Over curing of the first block would prevent bonding between the two blocks.

SEM and microscope images, as depicted in figure 4, showed evidence of the successful fabrication of the Janus particles. The SEM images clearly illustrate the biphasic architecture of

**Table 2.** The compositions of dipolar Janus particles.

	Wt%	Function
Bottom positive block in the mold		
PEG <sub>428</sub> triacrylate	87	Cross-linking agent
AEM	10	Positive charge
Fluorescein <i>o</i> -acrylate	2	Fluorophore
HCPK	1	Initiator
DMSO	10 $\mu$ l/100 mg monomer	Solvent
Isopropanol	200 $\mu$ l/100 mg monomer	Volatile solvent
Top negative block in the mold		
PEG <sub>912</sub> triacrylate	69	Cross-linking agent
PEG <sub>1000</sub>	20	Hydrophile
Acrylic acid	10	Negative charge
HCPK	1	Initiator
DMSO	10 $\mu$ l/100 mg monomer	Solvent

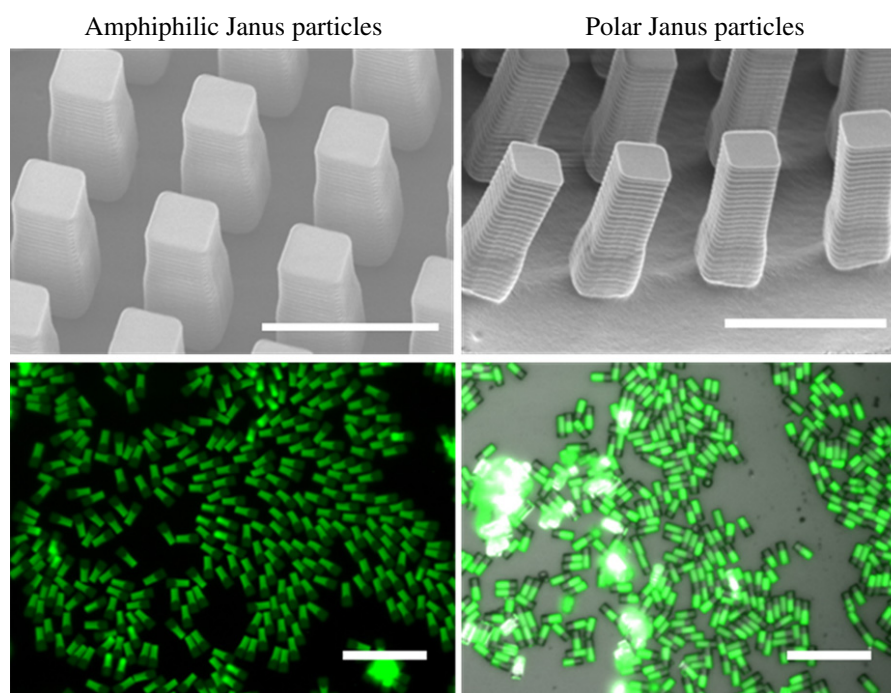


**Figure 4.** SEM (top) and microscope (bottom) images of amphiphilic (left) and dipolar (right) Janus particles. Particles in the SEM images were harvested on a polycyanoacrylate harvesting layer. The microscope image of the amphiphilic Janus particles was obtained from fluorescent channel and that of the dipolar Janus particles was from the overlaid image of fluorescent and bright field channels. The scale bars in the SEM images represent 5  $\mu$ m, and in the microscope images 20  $\mu$ m.

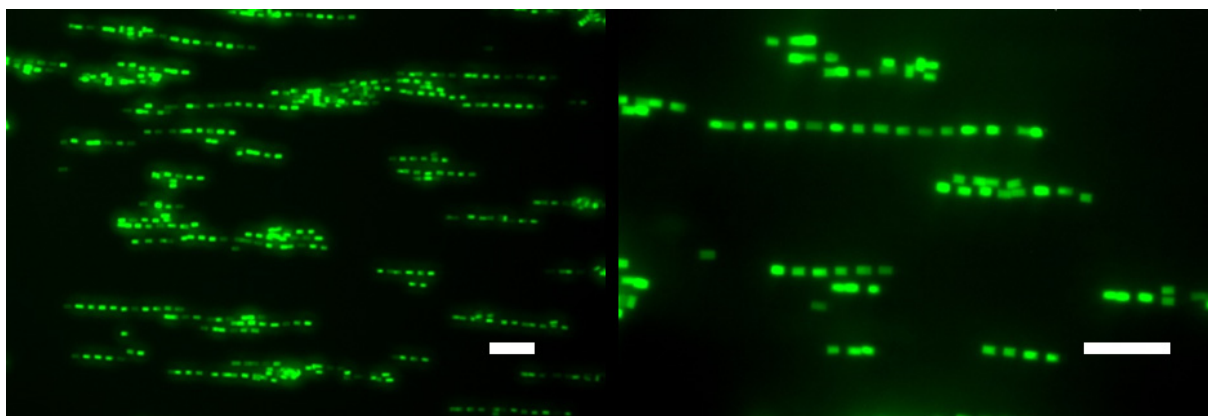


**Figure 5.** Fluorescence microscope images of dipolar Janus particles aligned in a  $250 \text{ V cm}^{-1}$  ac electric field. Note only one half of the particle fluoresces. Particles were dispersed in 1% Pluronic (non-ionic surfactant) aqueous solution. The scale bars represent  $20 \mu\text{m}$ .

the Janus particles, and in the fluorescence microscope images each Janus particle exhibited a fluorescent segment doped with fluorophore and a dark segment that did not contain a fluorophore.

Colloids that exhibit partial wettability with a pair of immiscible fluids can become trapped at interfaces between them and subsequently used as emulsifiers [38, 39]. Our unpublished results have shown that amphiphilic PRINT Janus particles can stabilize bicontinuous emulsions of a 2,6-lutidine/water system. The dipolar Janus particles also have been shown to demonstrate remote positioning in an electric field, as shown in figure 5, due to their dipole moment.

## 5. Multiphasic and regio-specifically functionalized particles

The fabrication methods introduced above can also be combined in a comprehensive process to create more complex particles, like the triphasic particles shown in figure 6. First,  $2 \times 2 \times 6 \mu\text{m}$  rectangular prism Janus particles, with compositions detailed in table 3, were cured in a mold with AEM in the top block of the mold as a chemical handle. In the second step, while the two-phase Janus particle was still in the mold, the exposed end was treated with NHS-rhodamine to yield red dye end-labeled triphasic particles.

Particles of a triphasic nature can also be fabricated by functionalizing both ends of PRINT particles. The first exposed face of the rectangular prism was functionalized as described in section 3.1. The particles were then removed from the mold using polycyanoacrylate, and a polystyrene protecting layer was cast onto the array from a 10 wt% solution of polystyrene in chlorobenzene. SEMs of the protected array are shown in figures 7(a) and (b). The newly exposed faces were then chemically modified with NHS-rhodamine. Both the protecting layer and the harvesting layer were dissolved, resulting in triphasic particles, where opposite faces of the prism were rhodamine functionalized (figure 7(c)).

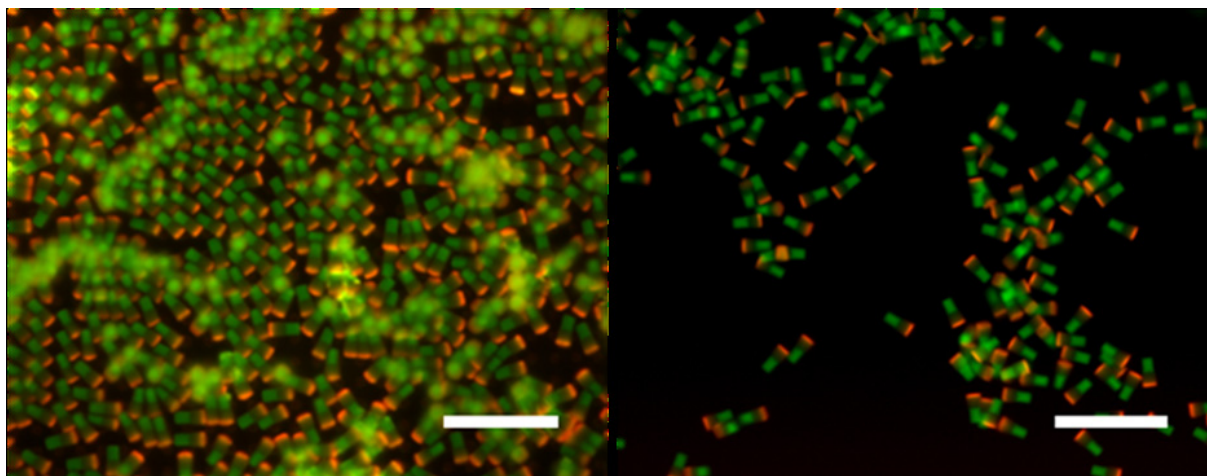


**Figure 6.** Fluorescence images of triphasic particles. Particles in the left image were collapsed on a polycyanoacrylate harvesting layer after a drop of acetone was applied. The right image shows purified, dried particles. The scale bars represent 20  $\mu\text{m}$ .

**Table 3.** The compositions of Janus particles. AEM in the top block was the chemical handle to be functionalized by reacting with NHS-rhodamine.

	Wt%	Function
Bottom hydrophobic block in the mold		
PEG <sub>428</sub> triacrylate	47	Cross-linking agent
Lauryl acrylate	50	Hydrophobe
Fluorescein <i>o</i> -acrylate	2	Fluorophore
HCPK	1	Initiator
DMSO	10 $\mu\text{l}/100$ mg monomer	Solvent
Isopropanol	200 $\mu\text{l}/100$ mg monomer	Volatile solvent
Top hydrophilic block in the mold		
PEG <sub>912</sub> triacrylate	74	Cross-linking agent
PEG <sub>1000</sub>	20	Stabilizer
AEM	5	Chemical handle
HCPK	1	Initiator
DMSO	10 $\mu\text{l}/100$ mg monomer	Solvent

## 6. Conclusions

Our previous reports have demonstrated that the PRINT technology is a highly versatile method for the production of particles with precisely controlled size, shape, matrix composition and cargo. In this work, we have added an extra parameter to the PRINT technology in order to achieve anisotropic distribution of matter within the particle: surface post-functionalization of PRINT particles embedded in the mold or the casting of a protecting layer gives rise to regio-specifically functionalized particles; filling and curing liquid monomer layers (theoretically it



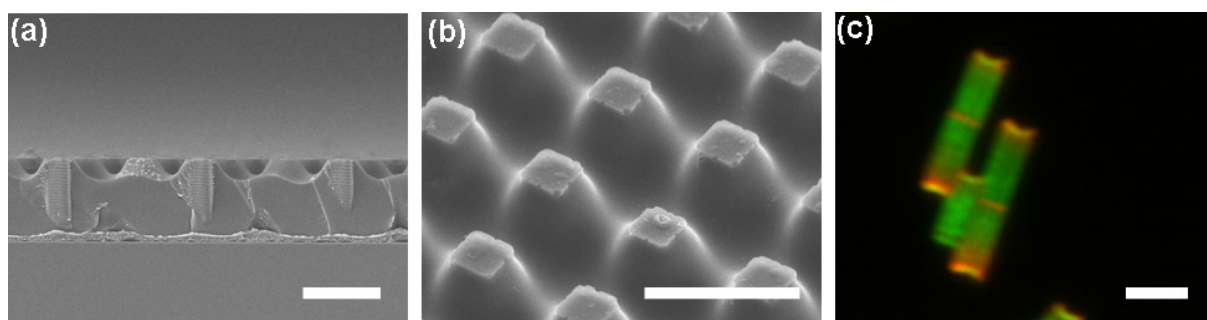


**Figure 7.** (a) Cross-sectional and (b) angled SEM views of the  $2 \times 2 \times 6 \mu\text{m}$  particle array on polycyanoacrylate with a polystyrene protection layer and (c) purified triphasic particles. Scale bars represent  $5 \mu\text{m}$ .

could be done multiple times) produces Janus particles; and in addition, the combination of these fabrication methods to construct sophisticated multiphase particles.

Owing to their unique characteristics, i.e. controlled phase separation and thus anisotropic functionality and property arrangement on the surface, these multiphase PRINT particles have shown promise for applications in life science and material science. End-capped particles have the capability for enhanced performance in drug-delivery, especially for cell internalization. Hydrophobic–hydrophilic Janus particles functioned as a stabilizer in water/oil emulsions. Dipolar Janus particles displayed a pronounced response to an ac electric field. Triphasic particles, such as the end-capped Janus particles and doubly end-capped particles, are more complex and versatile versions of the biphasic particles. These particles in particular hold great promise as multifunctional materials. These multiphase PRINT particles have great potential for numerous applications including multicomponent drug-delivery systems and directional self-assembly toward complex hierarchical assemblies and novel materials.

### Acknowledgments

We thank Liquidia Technologies for the hexnut replica and Fluorocur<sup>TM</sup> resin, Dr Patricia A Ropp for the cell work and confocal microscopy, Dr Douglas E Betts for useful discussions, Dr Gary Bordanero, Dr Robert Ilic and Dr Meredith Metzler of the Cornell Nanofabrication Facility who were instrumental in the fabrication of the  $2 \times 2 \times 6 \mu\text{m}$  patterned silicon masters. This work was supported by the STC program of the National Science Foundation (CHE 9876674), National Institutes of Health Program Project Grant PO1-GM059299, National Institutes of Health Grant U54-CA119343 (the Carolina Center for Cancer Nanotechnology Excellence), DARPA (07-4627), Liquidia Technologies, the Office of Naval Research N00014-08-1-0978 and the Chancellor's Eminent Professorship at the University of North Carolina at Chapel Hill.

## References

- [1] Davis M E, Chen Z and Shin D M 2008 Nanoparticle therapeutics: an emerging treatment modality for cancer *Nat. Rev. Drug Discov.* **7** 771–82
- [2] Euliss L E, DuPont J A, Gratton S and DeSimone J 2006 Imparting size, shape, and composition control of materials for nanomedicine *Chem. Soc. Rev.* **35** 1095–104
- [3] Teranishi T 2006 Anisotropically phase-separated biphasic particles *Small* **2** 596–8
- [4] Perro A, Reculosa S, Ravaine S, Bourgeat-Lami E B and Duguet E 2005 Design and synthesis of Janus micro- and nanoparticles *J. Mater. Chem.* **15** 3745–60
- [5] Gratton S E A, Pohlhaus P D, Lee J, Guo J, Cho M J and DeSimone J M 2007 Nanofabricated particles for engineered drug therapies: a preliminary biodistribution study of PRINT™ nanoparticles *J. Control. Release* **121** 10–8
- [6] Gratton S E A, Ropp P A, Pohlhaus P D, Luft J C, Madden V J, Napier M E and DeSimone J M 2008 The effect of particle design on cellular internalization pathways *Proc. Natl Acad. Sci. USA* **105** 11613–8
- [7] Gratton S E A *et al* 2008 The pursuit of a scalable nanofabrication platform for use in material and life science applications *Acc. Chem. Res.* **41** 1685–95
- [8] Hampton M J, Williams S S, Zhou Z, Nunes J, Ko D-H, Templeton J L, Samulski E T and DeSimone J M 2008 The patterning of sub-500 nm inorganic oxide structures *Adv. Mater.* **20** 2667–73
- [9] Herlihy K P, Nunes J and DeSimone J M 2008 Electrically driven alignment and crystallization of unique anisotropic polymer particles *Langmuir* **24** 8421–6
- [10] Kelly J Y and DeSimone J M 2008 Shape-specific, monodisperse nano-molding of protein particles *J. Am. Chem. Soc.* **130** 5438–9
- [11] Maynor Benjamin W *et al* 2007 Supramolecular nanomimetics: replication of micelles, viruses, and other naturally occurring nanoscale objects *Small* **3** 845–9
- [12] Petros R A, Ropp P A and DeSimone J M 2008 Reductively labile PRINT particles for the delivery of doxorubicin to HeLa cells *J. Am. Chem. Soc.* **130** 5008–9
- [13] Rolland J P, Maynor B W, Euliss L E, Exner A E, Denison G M and DeSimone J M 2005 Direct fabrication and harvesting of monodisperse, shape-specific nanobiomaterials *J. Am. Chem. Soc.* **127** 10096–100
- [14] Xia Y and Whitesides G M 1998 Soft lithography *Annu. Rev. Mater. Sci.* **28** 153–84
- [15] Xia Y N, Rogers J A, Paul K E and Whitesides G M 1999 Unconventional methods for fabricating and patterning nanostructures *Chem. Rev.* **99** 1823–48
- [16] Xia Y N and Whitesides G M 1998 Soft lithography *Angew. Chem., Int. Ed. Engl.* **37** 551–75
- [17] Glotzer S C and Solomon M J 2007 Anisotropy of building blocks and their assembly into complex structures *Nat. Mater.* **6** 557–62
- [18] Glotzer S C 2004 Some assembly required *Science* **306** 419–20
- [19] Braeckmans K, De Smedt S C, Leblans M, Pauwels R and Demeester J 2002 Encoding microcarriers: present and future technologies *Nat. Rev. Drug Discov.* **1** 447–56
- [20] Derveaux S, Stubbe B, Braeckmans K, Roelant C, Sato K, Demeester J and De Smedt S 2008 Synergism between particle-based multiplexing and microfluidics technologies may bring diagnostics closer to the patient *Anal. Bioanal. Chem.* **391** 2453–67
- [21] Zhang Z and Glotzer S C 2004 Self-assembly of patchy particles *Nano Lett.* **4** 1407–13
- [22] Cayre O, Paunov V N and Velev O D 2003 Fabrication of dipolar colloid particles by microcontact printing *Chem. Commun.* 2296–7
- [23] Cui J-Q and Kretzschmar I 2006 Surface-anisotropic polystyrene spheres by electroless deposition *Langmuir* **22** 8281–4
- [24] Hong L, Jiang S and Granick S 2006 Simple method to produce Janus colloidal particles in large quantity *Langmuir* **22** 9495–9
- [25] Paunov V N and Cayre O J 2004 Supraparticles and ‘Janus’ particles fabricated by replication of particle monolayers at liquid surfaces using a gel trapping technique *Adv. Mater.* **16** 788–91

- [26] Pawar A B and Kretzschmar I 2008 Patchy particles by glancing angle deposition *Langmuir* **24** 355–8
- [27] Yang S M, Kim S H, Lim J M and Yi G R 2008 Synthesis and assembly of structured colloidal particles *J. Mater. Chem.* **18** 2177–90
- [28] Zhang G, Wang D and Mohwald H 2006 Nanoembossment of Au patterns on microspheres *Chem. Mater.* **18** 3985–92
- [29] Takei H and Shimizu N 1997 Gradient sensitive microscopic probes prepared by gold evaporation and chemisorption on latex spheres *Langmuir* **13** 1865–8
- [30] Sundararajan S, Lammert P E, Zudans A W, Crespi V H and Sen A 2008 Catalytic motors for transport of colloidal cargo *Nano Lett.* **8** 1271–6
- [31] Casagrande C, Fabre P, Raphael E and Veyssie M 1989 Janus beads—realization and behavior at water/oil interfaces *Europhys. Lett.* **9** 251–5
- [32] De Gennes P G 1992 Soft matter *Science* **256** 495–7
- [33] Hong L, Cacciuto A, Luijten E and Granick S 2006 Clusters of charged Janus spheres *Nano Lett.* **6** 2510–4
- [34] Nisisako T, Torii T, Takahashi T and Takizawa Y 2006 Synthesis of monodisperse bicolored Janus particles with electrical anisotropy using a microfluidic co-flow system *Adv. Mater.* **18** 1152–6
- [35] Jiang S and Granick S 2007 Janus balance of amphiphilic colloidal particles *J. Chem. Phys.* **127** 161102
- [36] Roh K-H, Martin D C and Lahann J 2005 Biphasic Janus particles with nanoscale anisotropy *Nat. Mater.* **4** 759–63
- [37] Walther A and Muller A H E 2008 Janus particles *Soft Matter* **4** 663–8
- [38] Clegg P S 2008 Fluid-bicontinuous gels stabilized by interfacial colloids: low and high molecular weight fluids *J. Phys.: Condens. Matter* **20** 113101
- [39] Stratford K, Adhikari R, Pagonabarraga I, Desplat J C and Cates M E 2005 Colloidal jamming at interfaces: a route to fluid-bicontinuous gels *Science* **309** 2198–201